

# Digital Control of DSTATCOM using TI-C2000 Processor and MATLAB/ Simulink for Sustainable Power System Network

*K. Mahammad Rafi*<sup>1\*</sup>, *Vinay Kumar Awaar*<sup>2</sup>, *Phani Kumar K.S.V*<sup>3</sup>, *G Pradeep Reddy*<sup>4</sup>, *Sakshi Koli*<sup>5</sup>, *K Kalpana*<sup>6</sup>

<sup>1</sup>Muffakham Jah College of Engineering and Technology, Hyderabad, Telangana, INDIA.

<sup>2</sup>Gokaraju Rangaraju Institute of Engineering and Technology, Hyderabad, Telangana, INDIA.

<sup>3</sup>CVR College of Engineering, Ibrahimpatnam, Rangareddy, Telangana, INDIA.

<sup>4</sup>School of Electronics Engineering VIT-AP University, Amaravati, Andhra Pradesh, INDIA.

<sup>5</sup>Uttaranchal Institute of Technology, Uttaranchal University, Dehradun, 248007, INDIA.

<sup>6</sup>KG Reddy College of Engineering & Technology, Hyderabad, Telangana, INDIA.

**Abstract.** This paper describes the detailed digital control of a Distribution Static Synchronous shunt Compensator (DSTATCOM) using a MATLAB embedded coder for compensation to be in command of Voltage Source Converter (VSC) input voltage, reactive power compensation and the power factor improvement of a secondary radial distribution system with a voltage rating of 11kV/415V and with a capacity of 750 kW. The model has been simulated and tested in MATLAB/Simulink using the Simscape tool block set version of MATLAB R2019a. The same is achieved using a 32-bit DSP TMS320F2812 controller programmed with CCS V 6.1 software and tested with MATLAB embedded coder generation using Texas Instrument C2000 processors. Using this embedded code is developed and dumped into the CCS V 6.1. Real and Reactive power control (PQ) and Back Propagation Control Algorithm (BPCA) are the control methods. BPCA controller is based on the elementary extracted biased value of Reactive Power (Q) and Active Power (P) components of load currents. These current values are necessary for the reference source's current estimation. The reference source currents are estimated from the available source currents to generate firing pulses for the PQ and BPCA controllers. The real and reactive power controller is based on the transformation of synchronously rotating load currents in alpha and beta frames. The BPCA-based DSTATCOM is simulated for linear and non-linear load circumstances and that helps in restoring the power system networks sustainability.

## 1 Introduction

Reactive power control is significant today due to more non-linear loads being connected to Electrical Distribution System (EDS), so the system gets polluted due to the non-linear load on the load side [1-4]. The control of reactive power enables the system to get a better power factor (PF), which leads to a reduction in line current follow-on in proper consumption of the distribution transformer and reduced power bills. The complicated systems controlled using embedded coder are essential in the digital control design of any system. This can be achieved using MATLAB/Simulink and a CCS controller [5-8]. The

---

\* Corresponding author: [rafi.eee@mjcollege.ac.in](mailto:rafi.eee@mjcollege.ac.in)

excessive reactive power demand and harmonics in the system due to non-linear and variable loads diminish the distribution system's real power flow (P) and hence the sustainability. To overcome these problems, in this paper, fast, acting voltage source converter (VSC) input voltage control and reactive power control algorithms are studied and finally analyzed. The best suitable control methodology is proposed to DSTATCOM for reactive power compensation. By these controllers, the DSTATCOM would generate under voltage or over voltage at PCC, this lead to lagging or leading power factor at the bus. To avoid problems connected with lagging and leading pf and minimized harmonics in the system. The power factor can be kept at the desired level regardless of the system terminal voltage. These loads can be grouped as resistive, inductive type and some harmonic injecting variable type of non-linear loads. This paper deals with two major types of controls, as mentioned above.

The static synchronous compensator is connected parallel to a 3- phase load side, the connected source resistance and reactance, which are depicted in Fig. 1. The controller control performance depends upon the correctness of reactive power injection at the bus. The tuned values of the coupling reactor ( $L_f$ ) are connected to the ac output of the voltage source converter. The controller injects the required amount of currents to control the reactive power at the bus. The rating of injecting current at the bus decides the rating of the VSC. The choice of VSC input voltages, rating of coupling capacitor value, and interfacing reactor value are vital for controlling the VSC converter as a DSTATCOM control mode.

## 2 Control Philosophies of DSTATCOM

The primary control calculation of DSTATCOM is to estimate the necessary reference current signals from input signals received from the field. These reference current signals, alongside related detected current signals, are utilized in PWM current regulators to drive gating PWM signals for turning on the IGBTs of the VSC utilized as a DSTATCOM. Appropriately reference current signals must be inferred to control DSTATCOM, and these signals likely utilize various control calculations [9, 11, 12]. Numerous DSTATCOM control calculations are accounted for in the writing. The DSTATCOM control techniques are divided into two major groups; the first group belongs to the primary control techniques and the second to the adaptive control techniques [13].

### 2.1 Real and Reactive (PQ)

In the PQ control technique, signals are sensed from the field, processed, and analyzed [13-15]. The voltage signals of the a, b and c phases are represented as  $V_{sa}$ ,  $V_{sb}$  &  $V_{sc}$ , respectively. The source currents are represented as  $i_{sa}$ ,  $i_{sb}$  &  $i_{sc}$ . The input DC link capacitor voltage is  $V_{DC}$  and three inverter currents of  $i_{ir}$ ,  $i_{iy}$  &  $i_{ib}$ . The obtained current and voltage signals are converted into 3-phase to 2-phase quantities; by using these signals, real power ( $p_s$ ) and reactive power ( $q_s$ ) is calculated [9-10]. The PQ controller, a MATLAB/Simulink model, is shown in Fig. 2. The entire control power circuit of DSTATCOM is simulated in Simulink programming. The detailed real and reactive power flow equations and mathematical models are explained with vector diagrams and shown in Appendix-A.

### 2.2 Simulink model of PQ control

The source voltage and currents of the 3-phase system are represented as  $v_{sa}$ ,  $v_{sb}$ ,  $v_{sc}$  and  $i_{sa}$ ,  $i_{sb}$ , and  $i_{sc}$ , respectively. These voltage and currents are measured using ammeter and voltmeter measurement blocks in the Electrical/specialized power systems/ fundamental blocks/ measurements. The source's measured current and voltage signals are converted into equivalent  $\alpha$ - $\beta$  component values ( $i_\alpha$ ,  $i_\beta$ ;  $v_\alpha$ ,  $v_\beta$ ). These  $\alpha$ - $\beta$  component values

compute the useful power ( $p_s$ ) and reactive power ( $q_s$ ) supplied by the source to meet the load necessity. The mathematical relations used in the controller are given from Equation 1 to Equation 7. Standard nomenclature has been adopted for the parameters of the system.

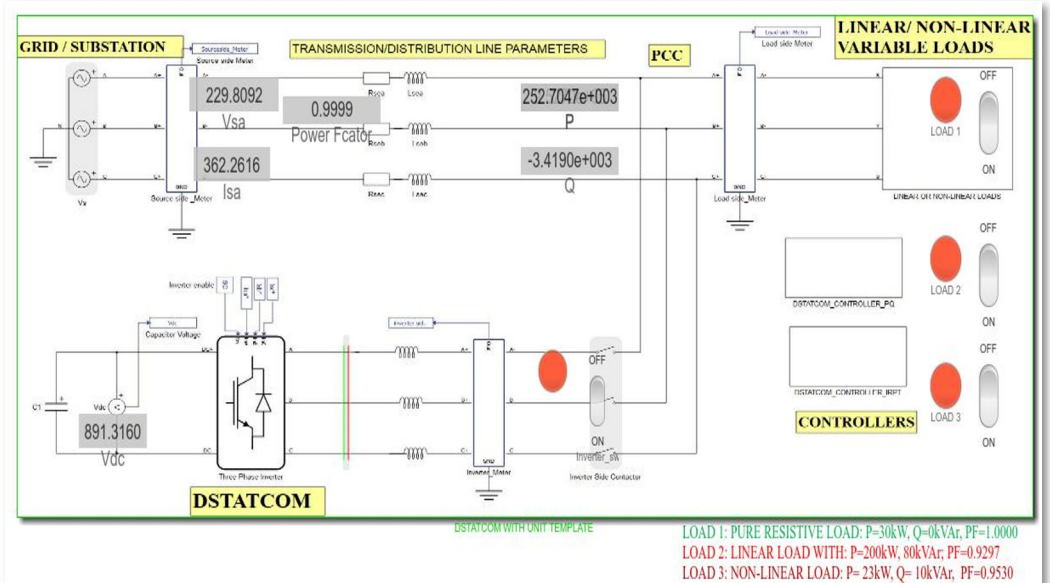


**Fig. 1.** DSTATCOM simulated model in MATLAB.

$$\begin{bmatrix} v_{s\alpha} \\ v_{s\beta} \end{bmatrix} = [C] \begin{bmatrix} v_{sa} \\ v_{sb} \\ v_{sc} \end{bmatrix} \quad (1)$$

$$\begin{bmatrix} i_{s\alpha} \\ i_{s\beta} \end{bmatrix} = [C] \begin{bmatrix} i_{sa} \\ i_{sb} \\ i_{sc} \end{bmatrix} ; \text{ where } [C] = \sqrt{\frac{2}{3}} \begin{bmatrix} 1 & -1/2 & -1/2 \\ 0 & \sqrt{3}/2 & -\sqrt{3}/2 \end{bmatrix} \quad (2)$$

$$\begin{bmatrix} p_s \\ q_s \end{bmatrix} = \begin{bmatrix} v_{s\alpha} & v_{s\beta} \\ -v_{s\beta} & v_{s\alpha} \end{bmatrix} \begin{bmatrix} i_{s\alpha} \\ i_{s\beta} \end{bmatrix} \quad (3)$$

The instantaneous 3-phase real power is calculated using Equations 4 and 5

$$P_{S3\phi} = [(V_{\alpha} \times i_{\alpha}) + (V_{\beta} \times i_{\beta})] \quad (4)$$

$$P_{S3\phi} = [(v_{sa} \times i_{sa}) + (v_{sb} \times i_{sb}) + (v_{sc} \times i_{sc})] \quad (5)$$

The 3- phase instantaneous reactive power calculations are given in Equations 6 and 7.

$$q_{S3\phi} = [(V_{\alpha} \times i_{\beta}) - (V_{\beta} \times i_{\alpha})] \quad (6)$$

$$q_{S3\phi} = \frac{1}{\sqrt{3}} [i_{sa}(v_{sc} - v_{sb}) + i_{sb}(v_{sa} - v_{sc}) + i_{sc}(v_{sb} - v_{sa})] \quad (7)$$

To keep up the drawn source reactive power ( $q_s$ ) as zero, the PWM converter output current flows should be controlled so that the converter provides the required reactive power magnitude ( $q_s$ ) along these lines. For the unity power factor in the system, the source delivers zero reactive power to the load.

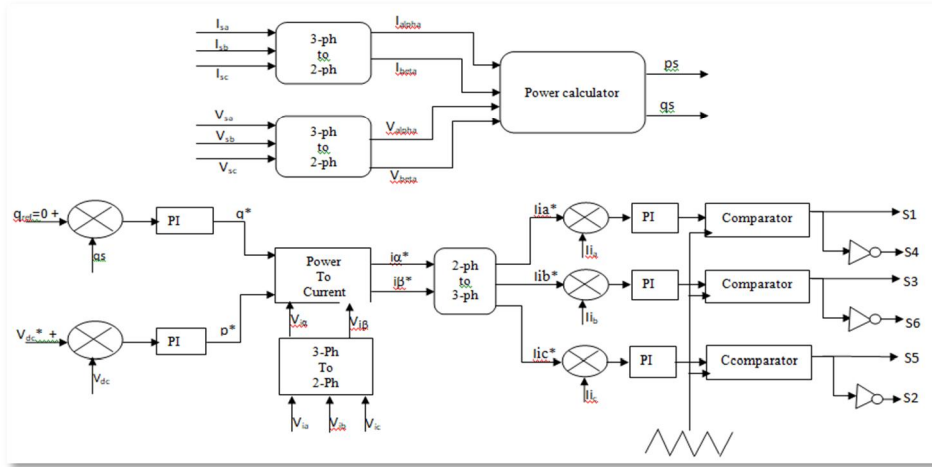


**Fig. 2.** Block diagram of PQ/IRPT control

In total compensation, the required reactive power ( $q_s$ ) provided by the supply is reduced from the reference value. The output error signal is supplied through a PI regulator block to obtain a reactive power signal, which is handled by the power to the current transformation block. This power-to-current transformation block needs real power and inverter voltages in  $\alpha$ - $\beta$  coordinates as contributions to compute the  $\alpha$ - $\beta$  component currents. In this, a self-controlled DC bus-fed converter is used. Consequently, the real power control signal ( $p^*$ ) will get from the VSC capacitor voltage regulator. The  $\alpha$ - $\beta$  segment currents from the power to current alteration block are fed to the 2-stage to 3-stage transformation block to get the 3-stage reference currents for the converter. The numerical relations for acquiring reference currents are given underneath. The current-regulated converter should generate these reference currents to maintain zero reactive power drawn from the source. To compensate for the reactive power in the system, the pulse width modulation approach is employed to provide the appropriate firing pulses. Fig. 2 depicts an IRPT control block diagram.

$$\begin{bmatrix} i_{i\alpha}^* \\ i_{i\beta}^* \end{bmatrix} = \frac{1}{v_{i\alpha}^2 + v_{i\beta}^2} \begin{bmatrix} v_{i\alpha} & v_{i\beta} \\ -v_{i\beta} & v_{i\alpha} \end{bmatrix} \begin{bmatrix} p^* \\ q^* \end{bmatrix} \tag{8}$$

$$\begin{bmatrix} i_{ia}^* \\ i_{ib}^* \\ i_{ic}^* \end{bmatrix} = [c]^T \begin{bmatrix} i_{i\alpha}^* \\ i_{i\beta}^* \end{bmatrix} \tag{9}$$

### 2.3 Hardware Model of PQ Control

The 3-phase primary line voltages and currents are measured through CT's & PT's; these signals are converted into control-level signals by using Hall Effect sensors of potential transformers, current transformers and signal training cards. These current and voltage signals of the source are first converted into the equivalent of  $\alpha$ - $\beta$  component values of ( $i_\alpha, i_\beta ; v_\alpha, v_\beta$ ). These  $\alpha$ - $\beta$  component values compute the real power/ useful power ( $p_s$ ) and reactive power ( $q_s$ ) supplied by the source to meet the load requirement. To keep the sustainable source delivered reactive power ( $q_s$ ) at zero, the PWM converter output currents should be regulated so that the converter supplies the reactive power of magnitude ( $q_s$ ). As a result, in the case of UPF at the source end, the source reactive power serves as the reference for the converter current control.

Digital signal processor (DSP) TMS320F2812 PGFQ board (LQFP-176) based control cards [6] and associated software have been used for phase conversions, reactive power and DC voltage control loops [8], [17-22], generation of reference current signals and some of the protections. Based on the current regulation scheme, analog and digital circuitry has been developed to produce PWM switching signals, delay in switching between top and bottom IGBTs and instantaneous current protection. The switching signals to the individual gate drives are transmitted through cables.

### 2.4 Back Propagation Control Algorithm (BPCA)

Fig. 3 depicts the backpropagation control algorithm block diagram. The weighted average values of the load real and reactive power current components can be used to determine reference source currents [16]. The phase a, b and c reference source currents are extracted using this controller. The point of common coupling voltages  $V_{sa}$ ,  $V_{sb}$ , and  $V_{sc}$ , load and source currents ( $i_{La}$ ,  $i_{Lb}$ ,  $i_{Lc}$ ,  $i_{sa}$ ,  $i_{sb}$ , and  $i_{sc}$ ) and DC link voltage  $V_{DC}$  are required in this backpropagation control technique is measured. This algorithm's primary modes of operation are feed-forward and reverse propagation errors.

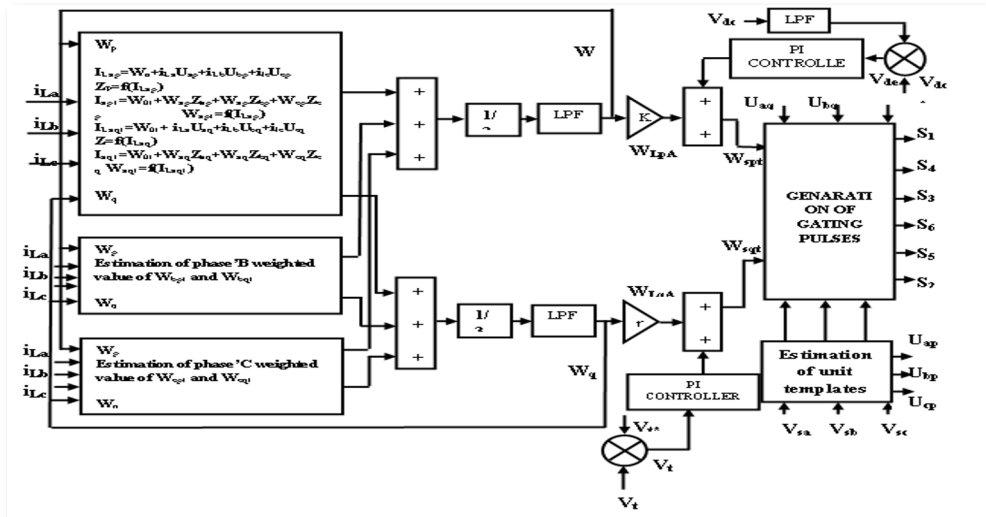


Fig. 3. Back Propagation Control Algorithm block diagram

## 3 Experimental setup specifications

The parameters listed below are utilized for both simulation and hardware modelling. The system has a capacity of 750 kW, and the incoming line is connected to two transformers of 500 kVA and 250 kVA. The system's total reactive power demand is around 300 kVar. Existing systems include two 150 kVar PFC banks; a 30 kVar DSTATCOM is proposed for additional power factor correction. (Based on existing 300 kVar PFC banks); AC power source: 3-phase, 415 V line voltage, 50 Hz;  $R_s$  of 0.05 Ohm and  $L_s$  of 2.1 mH (these values are obtained from cable ratings); The linear and non-linear loads are chosen. An educational institute's diverse motor loads, UPS, fan, and lighting load; The voltage source converter has a rating of 30 kVA. The inverter switching frequency is set to 2.5 kHz; the VSC input reference is set to 700 V; the DC bus capacitance ( $C_{dc}$ ) is set to 4700  $\mu\text{f}$  @ 450V; and the interfacing inductor (L<sub>f</sub>) is set to 3.6395 mH. VSC bus voltage proportional and integral (PI) controller gains:  $k_{id}$  is 0.9 and  $k_{pd}$  is 3.1.

## 4 Simulation Results

The system is modelled in this section as Control of DSTATCOM in PQ and BPCA with & without a fast-acting VSC PI controller. This part is examined the complete result analysis for various load circumstances without and with DSTATCOM for variable and fixed loads.

### 4.1 Case (a) Without Controller

In this section, the system is simulated without a controller with quarter, half, 3/4th, and full loads; the results of source current, active power, reactive power, and power factor are shown in Table 1.

**Table 1.** Test system parameters without controller

Type of load (RL) & Parameters	1/4 <sup>th</sup> LOAD	1/2 LOAD	3/4 <sup>th</sup> LOAD	FULL LOAD
source current (A) ( $I_s$ rms)	299.57	617.34	981.99	1357.90
Active Power (P) (kW)	199.32	400.58	599.46	800.07
Reactive Power (Q) (kVAr)	80.02	192.08	372.01	558.12
Power Factor (PF)	0.9329	0.901	0.8519	0.8216

Load variations of all four types of linear loads, switching at different time intervals using three-phase breakers, the base load are activated for the duration of the simulation, which is 2 seconds. Base load: 599.46 kW with a power factor of 0.8519. Load 1: 800.07 kW, 558.12 kVAr, 0.8216 power factors lagging, 0.4 to one second of duration Load 2: 400.58 kW, 192.08 kVAr, trailing power factor of 0.019, duration 0.7 to 1.2 seconds Load 3: 199.32 kW, 80.02 kVAr, trailing power factor of 0.9329, and duration of 1.3 to 1.7 seconds Fig. 4 depicts these variations.

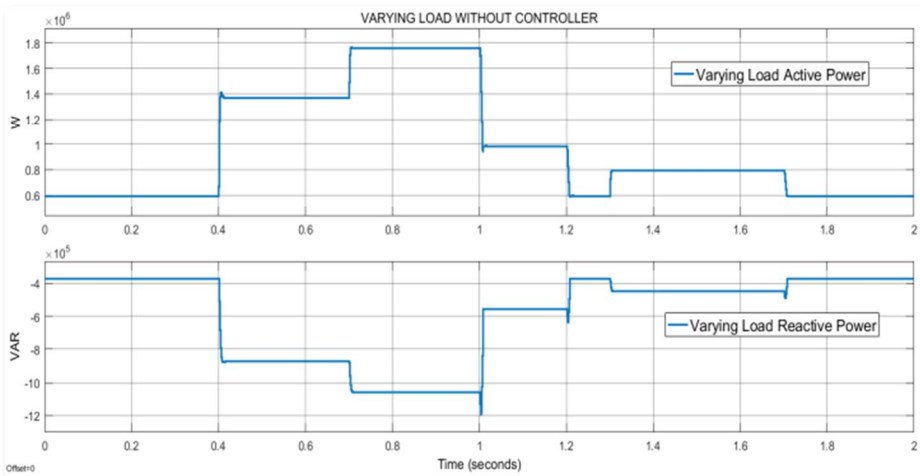


**Fig. 4.** Without controller real and reactive power of varying (step) load

### 4.2 Case (b) With the controller

The digital signal processor of the TMS320F2812 32-bit processor is used to execute the DSTATCOM controller, which is connected to a PC through a joint action group emulator and programmed using CCS V 6.1. The reactive power is calculated from the signals of current and voltage sensors using CCS programming. Using the previously mentioned

theories, such as PQ, the inverter stack should be fired, and the required amount of reactive power is injected into the bus to maintain the system power factor at unity. Fig. 5 depicts the Simulink model without a controller and a linear load. Fig. 6 depicts the whole hardware DSTATCOM model.

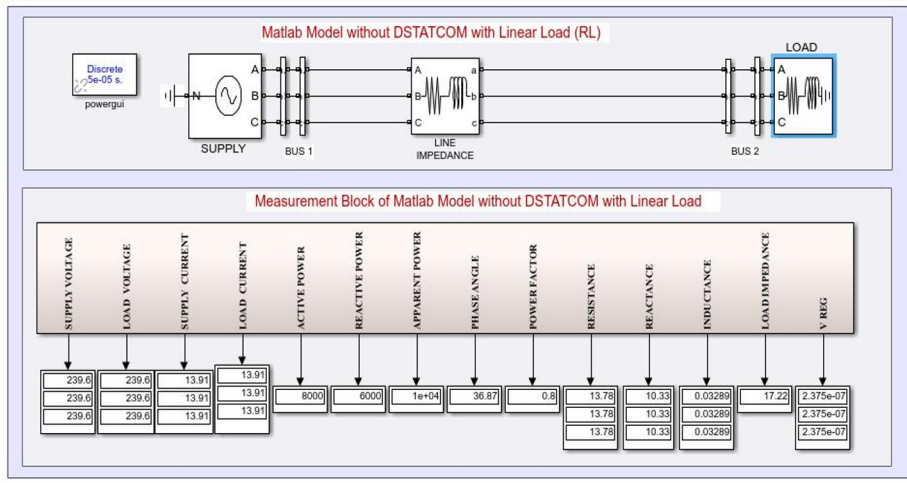


Fig. 5. Simulink model of the system without a controller with linear load

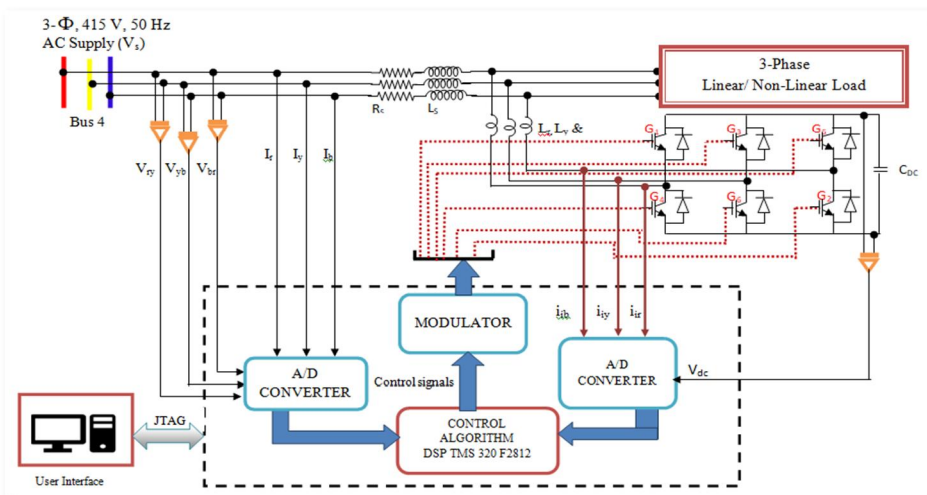
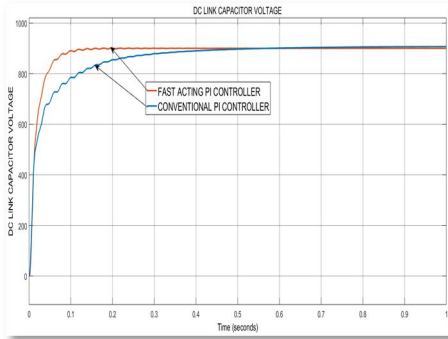


Fig. 6. Hardware model of PQ/IRPT control

Compared to a primary proportional plus integral controller, a fast-acting proportional plus integral (PI) controller has a shorter rise time, higher stability and fewer ripples. The various load changes were considered when developing this upgraded PI controller. A 25% of the load has been considered for that and it is shown in Fig. 7. The response times for traditional PI controllers have 506.95 milliseconds, and those of fast-acting PI controllers have 195.12 milliseconds when two different DC link voltages are applied on the same load for PQ. Fig. 8 depicts reactive power injections at 75% and 100% load. Fig. 9 and 10 depict variable load reactive and real powers and fluctuations in the angle between current and voltage in phase ‘a’ with 50% and 25% load without a controller. Without a controller, the phase angle between current and voltage in phase ‘a’ and the PF of the various loads

indicated in Table II are clearly shown. Fig. 11 and Fig. 12 demonstrate the PF correction and zero phase angles between voltage and current waveforms.



**Fig. 7.** A traditional and fast-acting PI controller

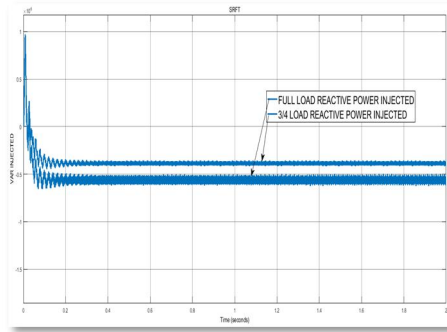


**Fig. 8.** Injections of reactive power at PCC for simulation of 3/4<sup>th</sup> full load

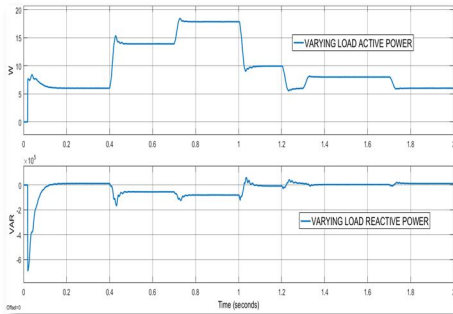


**Fig. 9.** After correction, BPCA real and reactive power on the bus

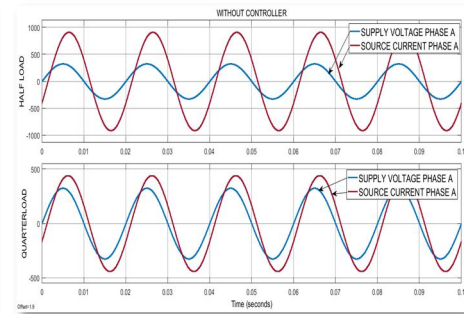


**Fig. 10.** Phase 'a' Voltage and current waveforms

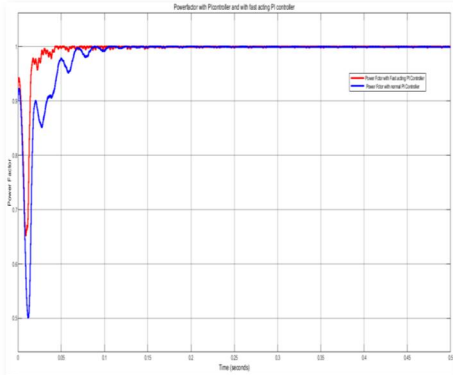


**Fig. 11.** Varying load power factor with Controller

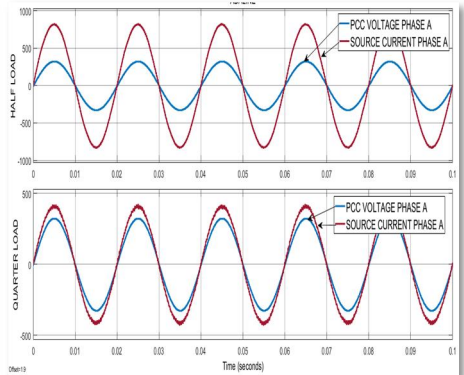


**Fig. 12.** Phase 'a' voltage and current wave forms with BPCA Controller

For non-linear load, the control of reactive power (Q), the load modelling and the PQ control are implemented in the CCS V6.1, and the DSP TMS 320 F2812 32-bit controller is used for control, the corresponding control firing pulses are observed in the GWINSTEK 2-Channel oscilloscope as shown in Fig. 13.



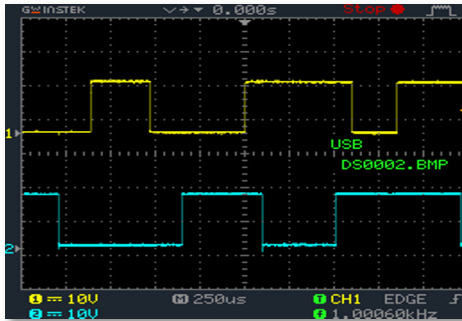


**Fig.13.** Firing pulses observed at one of instants in the oscilloscope

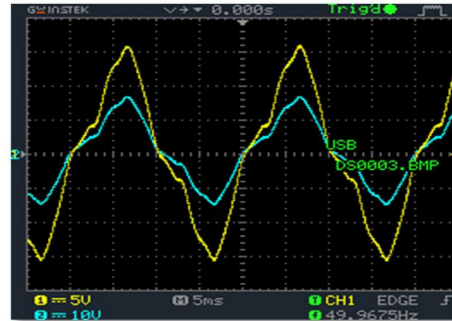


**Fig. 14.** Substation voltage and current waveform

The circuit depicted in Fig. 13 shows the firing pulses of the top and bottom switches of the first leg. The switches have a switching frequency of 1 kHz. Fig. 14. The substation voltage and current waveforms are shown for a load current of 98 A and a voltage of 236 V at an oscillation rate of 49.9 Hz. The detailed calculations are shown below. CT is 400/5 when connected to the 250 kVA transformer; the recorded peak voltage is 17.212 V and the primary current is computed as

$$I_p = \left\{ (CT \text{ Ratio}) \times \left( \frac{\text{Measured peak voltage}}{\sqrt{2}} \right) \times \left( \frac{1}{\text{Burden resis tan ce}} \right) \right\}$$

$$I_p = \left\{ \left( \frac{400}{5} \right) \times \left( \frac{17.2}{\sqrt{2}} \right) \times \left( \frac{1}{10} \right) \right\} = 97.29 \cong 98 \text{ A}$$

Power factors and correction time of different loading conditions with different controllers are shown in Table 2.

**Table 2.** Simulation results with PQ & BPCA controllers

Parameters	Without Control	PQ/IRPT	BPCA
<b>Quarter Load (200 kW)</b>			
Source current ( RMS)	300	278.39	278.35
Response period (ms)	-----	32	21
Power Factor	0.93	0.9992	0.9996
<b>Half load (400 kW)</b>			
Source current ( RMS)	617.25	554.77	556.7
Response period (ms)	----	75	45.98
Power Factor	0.9014	0.9992	0.9996
<b>3/4<sup>th</sup> load (600 kW)</b>			
Source current ( RMS)	982.25	1193.84	1193.37
Response period (ms)	---	58	43.99
Power Factor	0.8526	0.9996	0.9999
<b>Full load (800 kW)</b>			
Source current ( RMS)	1357.167	1112.89	1113
Response period (ms)	----	54	43.97
Power Factor	0.8256	0.9998	0.9988

## 5 Conclusions

In this paper, an 11kV/415V, 750 kW, 3-phase radial distribution system (RDS) was studied and the two DSTATCOM controllers were simulated in MATLAB/Simulink R2019a using embedded coder C2000 and successfully loaded the program in CCSV6.1 and tested. The fast-acting VSC input voltage is controlled using a modified proportional and integral controller and has been implemented and executed successfully. For linear and non-linear loads, parameters examined for analysis contain supply current, coupling voltage, real power, response period (milliseconds), injected reactive power and power factor. Verifying these results, an actual hardware model is executed with real and reactive power theory in DSP TMS 320F2812 for non-linear load, and the power factor of a test system is kept near unity and maintaining the sustainability using DSTATCOM. SPWM is used to generate the VSC gate firing pulses. Thus the simulation and experimental results PQ controller response time for power factor correction to non-linear and liner load is slightly slower than the BPCA controller.

The Authors gratefully acknowledge the support of the R&D Cell Muffakham Jah College of Engineering and Technology (MJCET), Road No. 03, Banjara Hills, Hyderabad, for their continuous inspiration, valuable suggestions, and financial support.

## References

1. B. Singh and J. Solanki, "A comparison of control algorithms for DSTATCOM," IEEE Trans. Ind. Electron., vol. **56**, no. 7, pp. 2738–2745, July (2009)
2. Kullan, M., Muthu, R., Mervin, J.B. and Subramanian, V. (2016) Design of DSTATCOM Controller for Compensating Unbalances. Circuits and Systems, 7, 2262-2272.
3. Power Quality Enhancement Using Custom Power Devices by Arindam Ghosh and Gerard Ledwich, (Kluwer academic publishers 2002).
4. Power quality problems and mitigation techniques by Bhim Singh, Ambrish Chandra and Kamal-Al-Haddad, (John Wiley and Sons Ltd 2015).
5. Understanding FACTS: Concepts and technology of flexible ac transmission systems by Narain G. Hingorani and Laszlo Gyugyi
6. MATLAB. 9.6.0.1072779 (R2019a). Natick, Massachusetts: The Math Works Inc.; 2019.
7. Texas Instruments Incorporated, "TMS320F2810-TMS320F2812 Digital Signal Processors Data Manual,".
8. Texas Instruments Incorporated, "Implementation of PID and Deadbeat Controllers with the TMS320 Family," Application Port: SPRA083.
9. B. Singh and J. Solanki, "A comparative study of control algorithms for DSTATCOM for load compensation," Proc. IEEE ICIT, (December 2006), pp. 1492-1497.
10. M. Kullan, R. Muthu, J. B. Mervin, et V. Subramanian, "Design of DSTATCOM Controller for Compensating Unbalances," Circuits Syst., vol. **07**, No 09, (2016). pp. 2362-2372.
11. Benhabib, MC and Saadate, S. (2005) New control approach for four-wire active power filter based on the use of synchronous reference frame. Electric Power Systems Research, **73**(3), pp. 353–362.
12. B. Singh and J. Solanki, "A comparative study of control algorithms for DSTATCOM for load compensation", Proc. IEEE ICIT, pp. 1492-1497, (2006-December)

13. Rafi, K.M., and Prasad, P.V.N. "Design and development of 30 kVAr DSTATCOM for reactive power compensation in an 800 kW radial distribution system", ARPN Journal of Engineering and Applied Sciences, Vol. **15**(12), pp. 1346–1354, (June-2020).
14. Singh, B., Adya, A., Mittal, A.P. and Gupta, J.R.P. (2005) Modeling and control of DSTATCOM for three-phase, four-wire distribution systems, Proceedings of the IEEE Industry Applications Society (IAS) Annual Meeting, October, vol. **4**, pp. 2428–2439.
15. Bhim Singh and Sabha Raj Arya "Backpropagation Control Algorithm for Power Quality Improvement Using DSTATCOM". Vol. **61**, No. 3, (March 2014).
16. Jung and G. N. Wang, "Pattern classification of backpropagation algorithm using exclusive connecting network," J. World Acad. Sci., Eng. Technol., vol. **36**, pp. 189–193, (December 2007).
17. Awaar, V.K., Jugge, P. & Tara Kalyani, Validation of Control Platform Using TMS320F28027F for Dynamic Voltage Restorer to Improve Power Quality, S. Journal of Control Automation and Electrical Systems, **30**, no.4, pp 601-610, (2019).
18. Awaar, Vinay Kumar, Praveen Jugge, S. Tara Kalyani, and Mohsen Eskandari *Dynamic Voltage Restorer—A Custom Power Device for Power Quality Improvement in Electrical Distribution Systems*, In Power Quality: Infrastructures and Control, pp. 97-116. Singapore: Springer Nature Singapore, (2023).
19. Awaar, Vinay Kumar, Neelima Jampally, Haritha Gali, and Rajshri Simhadri. "Real-Time BLDC Motor Control and Characterization Using TMS320F28069M with CCS and GUI." In *2022 IEEE 2nd International Conference on Sustainable Energy and Future Electric Transportation (SeFeT)*, pp. 1-6. IEEE, (2022).
20. Awaar, Vinay Kumar, Rajshri Simhadri, and Praveen Jugge. "Comparative Study And Experimentation of Speed Control Methods of BLDC Motor using DRV8312." In *2022 IEEE 2nd International Conference on Sustainable Energy and Future Electric Transportation (SeFeT)*, pp. 1-6. IEEE, (2022).
21. Phani Kumar K.S.V. and S Venkateshwarlu. "*Integrated operation of distributed resources to enhance frequency regulation in an isolated microgrid environment*," International Journal of Recent Technology and Engineering, 8:7479–7487, (2019).
22. Phani Kumar K.S.V. and S. Venkateshwarlu. "*Fuzzy controller based reserve management in hybrid microgrid for frequency regulation*," International Journal of Engineering and Advanced Technology, 9:652–663, (2019).
23. Karthik Rao, R., Bobba, P.B., Suresh Kumar, T., Kosaraju, S. "*Feasibility analysis of different conducting and insulation materials used in laminated busbars*" Materials Today: Proceedings, 26, pp. 3085-3089, (2019).
24. Tummala, S.K., Bobba, P.B., Satyanarayana, K. "*SEM & EDAX analysis of super capacitor*", Advances in Materials and Processing Technologies, 8 (sup4), pp. 2398-2409, (2022).
25. Tummala, S.K., Kosaraju, S. SEM analysis of grid elements in mono-crystalline and poly-crystalline based solar cell Materials Today: Proceedings, 26, pp. 3228-3233, (2019).
26. Nayak, P., Swetha, G.K., Gupta, S., Madhavi, K. *Routing in wireless sensor networks using machine learning techniques: Challenges and opportunities*, Measurement: Journal of the International Measurement Confederation, 178, art. no. 108974, (2021).
27. Nayak, P., Vathasavai, B. *Genetic algorithm based clustering approach for wireless sensor network to optimize routing techniques*, Proceedings of the 7th International Conference Confluence 2017 on Cloud Computing, Data Science and Engineering, art. no. 7943178, pp. 373-380, (2017).

28. V. Tejaswini Priyanka, Y. Reshma Reddy, D. Vajja, G. Ramesh and S. Gomathy (2023). *A Novel Emotion based Music Recommendation System using CNN*. 2023 7th International Conference on Intelligent Computing and Control Systems (ICICCS), Madurai, India, 592-596, doi: 10.1109/ICICCS56967.2023.10142330, (2023).
29. P. Singh, R. Shree, and M. Diwakar, *Journal of King Saud University - Computer and Information Sciences* 33, 313 (2021).